

Microstructure and Corrosion Properties of Calcium Phosphate Coating on Magnesium Alloy Prepared by Hydrothermal Treatment at Various pH Values

Zhang Chunyan^{1,2}, Zhang Shiyu¹, Liu Xinpeng¹, He Hongchuan¹

¹ Chongqing University of Technology, Chongqing 400054, China; ² Chongqing Municipal Engineering Research Center of Institutions of Higher Education for Special Welding Materials and Technology, Chongqing 400054, China

Abstract: Calcium phosphate (Ca-P) coatings were deposited on AZ31 magnesium by hydrothermal treatment at various pH values to improve the corrosion resistance and biocompatibility of magnesium alloys. The crystal phase, morphology and composition of the coatings were investigated by XRD, SEM and EDS, respectively. Electrochemical measurements and immersion tests were performed in Hank's solution to examine the bio-corrosion behaviors of the coated specimens. The results show that the pH value of solutions influences the phase composition and microstructure of the coating. And the degree of protection provided by the Ca-P coating varies with its microstructure. The deposited Ca-P coating treated at pH=6 is composed of OCP ($\text{Ca}_8\text{H}_2(\text{PO}_4)_6 \cdot 5\text{H}_2\text{O}$). When the pH value increases to 8 and 10, only the HA is formed. The HA coating with nano-scale and rod-like crystals prepared at pH=10 can prevent the penetration of solution more effectively than the OCP coating at pH=6 and the honeycomb-like HA coating at pH=8.

Key words: Ca-P coating; magnesium alloy; hydrothermal deposition; corrosion property; biomaterial

Magnesium alloys have become promising biodegradable bone implant materials owing to their good biocompatibility and the fact that their mechanical properties such as density and Young's modulus are close to those of human bones^[1-3]. However, magnesium alloys are extremely vulnerable to body fluid corrosion, resulting in pockets of hydrogen gas near the implant, increasing the alkalinity and magnesium ion concentration in the embedded surroundings, and prematurely reducing the mechanical properties of implants^[4-6], which prevents their further clinical use. Therefore, extensive studies related to enhancing the corrosion resistance and controlling the degradation time of magnesium alloys to match the rate of healing or regeneration of damaged bone have been performed over the last decade^[7-9].

Coating the base materials is a potentially effective way to acquire a moderate degradation rate adapted to the fracture healing process. In recent years, calcium phosphate coatings, including Hydroxyapatite (HA), β -tricalcium phosphate

(β -TCP), dicalcium phosphate dihydrate (DCPD) octacalcium phosphate (OCP) and Ca-deficient HA^[10-14], have been employed to improve the corrosion resistance and bone conductivity of magnesium-based alloys by ion beam assisted deposition^[15], micro-arc oxidation^[16], electrodeposition^[17,18], biomimetic^[19] and hydrothermal deposition^[20]. Among these methods, hydrothermal deposition is a simple and the least expensive way, and it can form coatings regardless of the substrate shape. Moreover, the treatment needs only a single step of immersion^[20-22].

It has been reported that the crystal shape, size and the crystallographic orientation of synthesized HA particles or flakes affect biological properties^[23,24]. Hiromoto has investigated the corrosion behavior of the Ca-P coated AZ31 by the immersion and polarization tests in 3.5 wt% NaCl solution^[12,21,22]. It was revealed that the degree of protection provided by calcium phosphate-coating varies with its crystal phase and microstructure^[12]. But the corrosion behavior in

Received date: October 08, 2017

Foundation item: National Natural Science Foundation of China (51201192)

Corresponding author: Zhang Chunyan, Ph. D., Associate Professor, School of Materials Science & Engineering, Chongqing University of Technology, Chongqing 400054, P. R. China, Tel: 0086-23-62563178, E-mail: zhangchunyan@cqut.edu.cn

Copyright © 2018, Northwest Institute for Nonferrous Metal Research. Published by Elsevier BV. All rights reserved.

NaCl is obviously different from that in simulated body fluid. In this study, the influence of the pH values of hydrothermal solutions on the phase structure and morphology of calcium phosphate coatings was investigated, and their biodegradation properties were evaluated by immersion tests and electrochemical measurement techniques (polarization and EIS tests) in Hank's solution.

1 Experiment

1.1 Sample preparation

Hot extruded AZ31 magnesium alloy sheets, 15 mm×15 mm×2 mm in dimension, were used as substrate materials. All specimens were ground with SiC abrasive paper up to 1000 grits, then cleaned in distilled water and dried at room temperature.

A hydrothermal treatment solution was prepared with ethylene diamine tetraacetic acid calcium disodium salt hydrate (Ca-EDTA) and potassium dihydrogen phosphate (KH₂PO₄). The concentration of the Ca-EDTA and KH₂PO₄ treatment solution was 0.25 mol/L. The pH of the solution was adjusted to 6, 8 and 10 with 0.1 mol/L NaOH solution. The AZ31 sheet was immersed in a separate Teflon container with solutions of various pH values at room temperature. Then the containers were placed in an oven at 363 K for 4 h.

1.2 Electrochemical measurement

The bio-corrosion resistance was evaluated by electrochemical tests using EG&G 273 type potentiostat in Hank's solution. The electrochemical measurements were carried out in a classical three-electrode cell with platinum as the counter electrode, saturated calomel electrode (SCE) as the reference electrode and hydrothermally treated AZ31 specimen as the working electrode. As a comparison, an as-polished AZ31 magnesium alloy sheet was also used. The specimen was first immersed in Hank's solution for 10 min to acquire a stable open circuit potential (OCP). Then EIS was performed on the OCP in the frequency range from 100 kHz to 0.01 Hz with an IM6e impedance system. The potentiodynamic polarization curve of the same sample was measured subsequently at a scan rate of 0.5 mV/s. The EIS results were fitted and analyzed using Zsimp Win software. The corrosion currents were calculated by Tafel extrapolating.

The chemical composition of Hank's solution includes: NaCl: 8 g/L, KCl: 0.4 g/L, CaCl₂: 0.14 g/L, NaHCO₃: 0.35 g/L, C₆H₆O₆: 1.0 g/L, MgCl₂·6H₂O: 0.1 g/L, MgSO₄·7H₂O: 0.06 g/L, KH₂PO₄: 0.06 g/L, Na₂HPO₄·12H₂O: 0.06 g/L.

1.3 Immersion test

The volume of hydrogen evolution is related to the dissolution rate of magnesium. Thus corrosion behavior of the specimen was measured by the hydrogen evolution test. The testing equipment were introduced in Ref.[18]. The AZ31 sheet and the hydrothermally treated AZ31 specimens were immersed vertically in Hank's solution for 15 d at room temperature (20~25 °C).

1.4 Surface characterization

The surface morphology of the hydrothermal coatings at various pH values before and after immersion in Hank's solution was characterized by scanning electron microscopy (SEM). The attached energy dispersive X-ray spectroscopy system (EDS) was used to examine the chemical composition. The structure of the coatings was analyzed by X-ray diffraction (XRD).

2 Results and Discussion

2.1 Microstructure of the coatings

Fig.1 shows the SEM images of the hydrothermally treated specimens at various pH values. Fig.1a displays that the surface of hydrothermally treated AZ31 alloy at pH=6 is fully covered with bract-like aggregates. Every bract-like structure consists of lamellar crystals of about 20 μm in length. The lamellar crystallites of the coating interlace together and form micro-pores. On the pH=8-treated AZ31, flocculent precipitates cover the surface uniformly and densely. The size of the flocculent precipitate is about a few microns. Observed at a high magnification, the flocks present a honeycomb structure (Fig.1b). On the pH=10-treated AZ31, the surface of specimen is densely covered by dandelion-like aggregates of rod-like crystals. The rod-like crystals are uniform and grow almost vertically from the inner substrate (Fig.1c). Fig.1 shows that the crystal size of the coatings treated at pH=8 and pH=10 is much finer than that of specimens treated at pH=6. The pore size of the coatings treated at pH=8 and pH=10 is only in a range of tens to hundreds nanometers.

Surface composition of the specimens obtained by EDS is summarized in Table 1. The coatings on all specimens are rich in Ca, P and O. Mg is not detected in the specimen treated at pH=6, while specimens treated at pH=8 and pH=10 contain 8.98 at% and 3.16 at% of Mg, respectively, indicating that the coating formed at pH=6 is thicker. In addition to the elements Ca, P and O, a small amount of Na probably from Ca-EDTA solution is detected on the surface of all hydrothermally treated specimens. Fig.2 shows the XRD patterns of the specimens. On the pH=6-treated AZ31, diffraction peaks from OCP (Ca₈H₂(PO₄)₆·5H₂O) and a sharp peak at 2θ=53.65° from Mg₃(PO₄)₂ are observed in addition to the peaks from substrate AZ31. When the pH value increases to 8, only the HA (Ca₁₀(PO₄)₆(OH)₂) peaks are observed. On the pH=10-treated AZ31, the HA peaks are sharper than that of the pH=8 treated specimen, suggesting that the crystallinity of HA on the pH=10-treated specimen is higher. On all the hydrothermally treated specimens, the peak of (002)_{HA} or (002)_{OCP} is higher than that of the other peaks, indicating that the (002) plane of HA or OCP is oriented^[21,22].

Mg dissolves on the substrate surface in a hydrothermal environment at pH=6 and reacts with water to produce Mg(OH)₂ and hydrogen:



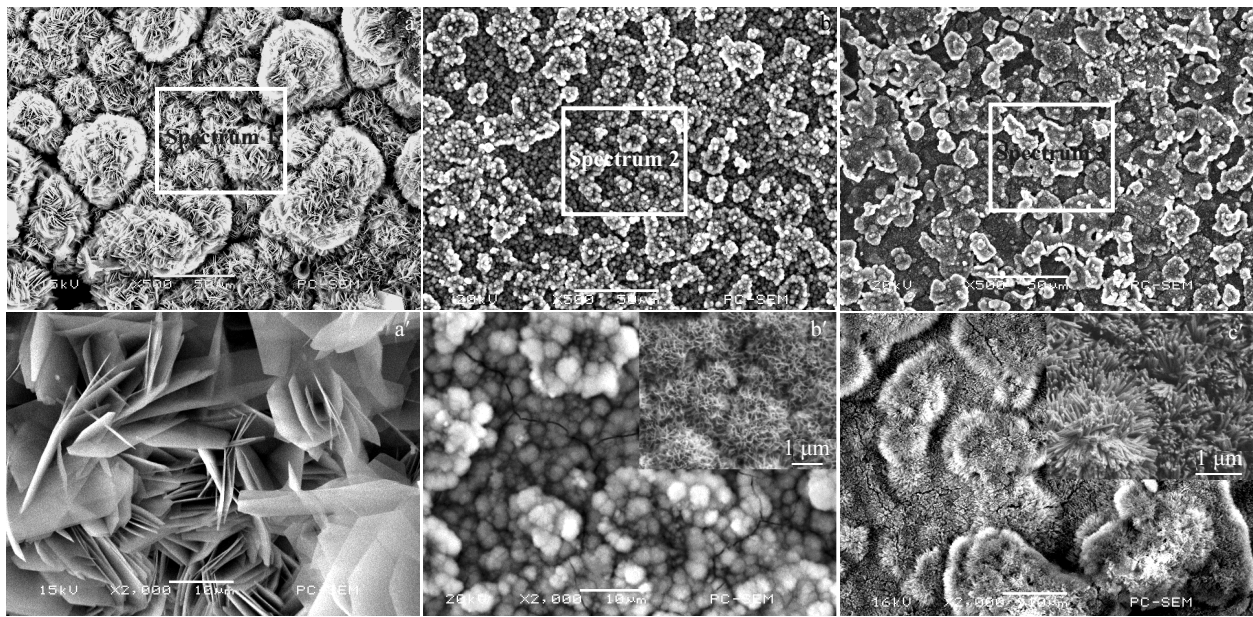


Fig.1 SEM images of the hydrothermally deposited coatings on AZ31 alloy at various pH values with different magnification: (a, a') pH=6, (b, b') pH=8, and (c, c') pH=10

Table 1 Chemical composition of the marked areas in Fig.1

Spectrum	O/at%	Mg/at%	Na/at%	P/at%	Ca/at%	Ca/P
1	79.59		1.51	9.09	9.81	1.08
2	51.63	8.98	3.11	15.44	20.84	1.35
3	55.52	3.16	2.42	16.16	22.74	1.41

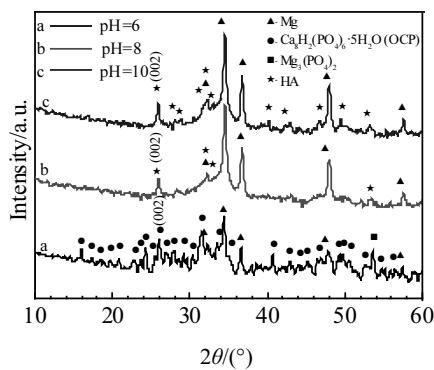


Fig.2 XRD patterns of AZ31 samples hydrothermally treated at various pH values

The rapid corrosion of magnesium raises the concentration of OH⁻ on the substrate surface regardless of the pH of the bulk treatment solution. The OH⁻ interacts with phosphate anions as follows:

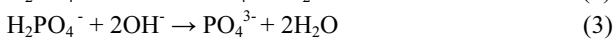
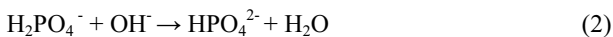
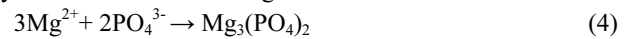
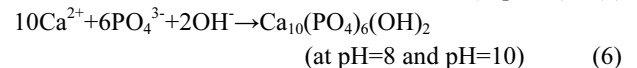
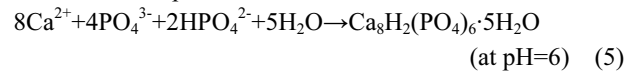


Table 1 shows that Mg is not detected on the surface of pH6- treated specimen, but a peak of Mg₃(PO₄)₂ is observed

in the XRD pattern (Fig.2a). It is thus revealed that following reaction maybe happen on AZ31 substrate at the initial hydrothermal treatment stage:



The rapid adsorption of HPO₄²⁻ and PO₄³⁻ on the sample surface produces a negatively charged surface and leads to the initial nucleation of calcium phosphate species. The initially precipitated calcium phosphate covers the surface, which behaves as a protective layer for separating the magnesium substrate from the treatment solution. The formation process of calcium phosphate coatings can be described by a combination of several reactions, including acid-base reaction, precipitation reaction and crystallization process^[25,26]. The reactions in the 0.25 mol/L Ca-EDTA and 0.25 mol/L KH₂PO₄ solution can be expressed as:



The type of calcium phosphate formed is closely dependent on the degree of supersaturation and the pH value of the solutions. At lower pH, DCPD and OCP may be involved as a precursor phase of HA^[26]. It is thus revealed that the pH value of the treatment solution should be controlled to be neutral to avoid co-precipitation of a large amount of OCP and Mg₃(PO₄)₂. It is reported that magnesium ions markedly inhibit the HA crystal growth in a solution supersaturated only with respect to this phase^[27]. Fig.1b and Fig.1c show that the crystals of HA are relatively fine, below 100 nm. The full width at half maximum of the (002)_{HA} peak in Fig.2b and

Fig.2c is 0.235 and 0.208, respectively. Calculated by Scherrer Equation, the size of crystals of HA formed under alkaline conditions is only about a few nanometers.

Table 1 shows that the Ca/P atomic ratio of the HA coating is lower than the theoretical value of HA (the Ca/P ratio of HA is 1.67), because the Ca in the HA structure is substituted with the Na atoms in the Ca-EDTA solutions.

2.2 Bio-corrosion properties of the coatings

2.2.1 Electrochemical behavior

The polarization curves of specimens in Hank's solution are shown in Fig.3. The electrochemical parameters fitted from the polarization curves are listed in Table 2. The polarization curves of all the coated samples display distinct passivation regions. Although the E_{corr} (corrosion potential) values of the hydrothermally treated specimens are lower than that of the AZ31 substrate, the E_{bk} (breakdown potential) is much higher than that of the AZ31 substrate, which indicates that the hydrothermally deposited coatings provide effective protection for magnesium alloys. Table 2 shows that the i_{corr} (corrosion current density) of the pH=6-treated specimen is very close to that of the AZ31 substrate. While the i_{corr} values of the pH=8 and pH=10-treated specimens are nearly 10 times lower than that of the AZ31 substrate. Among the hydrothermally treated specimens, the OCP coated specimen treated at pH=6 has the highest E_{bk} , indicating that the formed coating protects the substrate more effectively than the other two coated specimens. However, i_{corr} of OCP coated specimens is the highest, which suggests that when the coating is broken, the corrosion rate will be faster than that of other coated specimens. The E_{bk} of pH=10-treated specimen is close to that of the pH=8-treated specimen, but the i_{corr} is slightly lower.

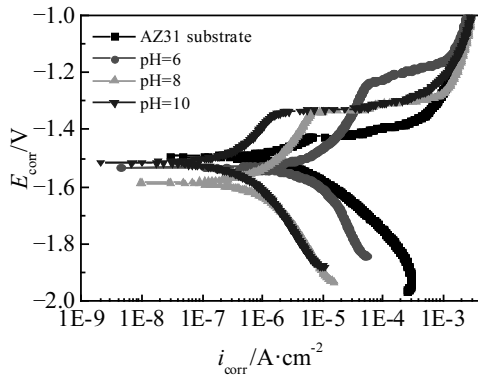


Fig.3 Polarization curves of AZ31 substrate and hydrothermally treated AZ31 at various pH values in the Hank's solution

Table 2 Parameters obtained from the polarization curves in Fig.3

Sample	E_{corr}/V	$i_{corr}/\times 10^{-6} A\cdot cm^{-2}$	E_{bk}/V
AZ31	-1.49	6.01	-1.42
pH=6-treated	-1.42	6.62	-1.24
pH=8-treated	-1.58	0.947	-1.34
pH=10-treated	-1.52	0.606	-1.35

Fig.4 shows the EIS plots of the specimens in the Hank's solutions. The EIS data for the specimens are fitted with equivalent circuits shown in Fig.5. Simulated data are shown in Table 3. The EIS plot of the uncoated AZ31 alloy in Fig.4a exhibits two capacitance loops at high and medium frequencies and one inductance loop at low frequencies. The equivalent circuit consists of electrolyte resistance (R_s), passivation film resistance (R_f), capacitance (Q_1), charge transfer resistance (R_{ct}), capacitance (Q_2), corrosion product inductance (L) and corrosion product resistance (R_L). The inductance loop is usually related to adsorption-desorption of ions^[28], so the existence of inductance loop indicates that the nucleation of corrosion pits forms on the uncoated AZ31 alloy. The Nyquist plots of the hydrothermally treated specimens show two capacitance loops at high and medium frequencies. Therefore, the system of the coated specimens can be viewed as a tandem circuit that is composed of R_s , coating resistance (R_f), Q_1 , R_{ct} and Q_2 . The value of R_s is usually small and has no effect on the coated system. The capacitance loops are related to the corrosion behavior and coating capacitance of the specimen. Barrier properties of the coating can be evaluated by the value of R_f , and coatings with less defects and high thickness will have a large value of R_f . The R_f of pH=6-treated AZ31 (7078 Ω) is higher than that of AZ31 with passivation film (4343 Ω),

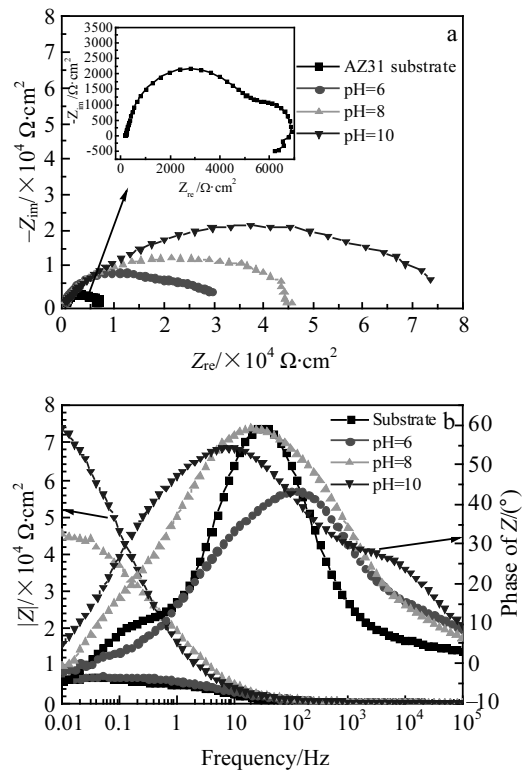


Fig.4 EIS plots of AZ31 magnesium alloy and hydrothermally deposited coatings on AZ31 at various pH values in Hank's solution: (a) Nyquist plots and (b) Bode plots

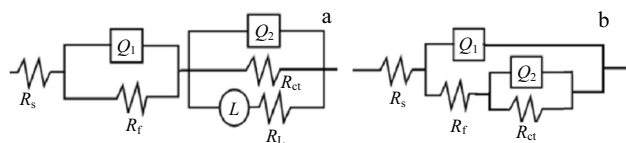


Fig.5 Equivalent circuits for electrode surface corrosion in Hank's solution: (a) AZ31, R(QR)(Q(RL)); (b) hydrothermally treated specimens, R(QR)(QR)

but much lower than that of pH=8 and pH=10-treated AZ31 (45210 Ω and 77950 Ω , respectively). The reason may be that the micro-pores of the coating on pH=6-treated AZ31 specimen leads to a decrease in its resistance. The R_{ct} value reflects the difficulty of the electrochemical corrosion reaction. The R_{ct} values of the hydrothermally treated samples are much lower than that of untreated AZ31 (2252 Ω), indicating that electrons are easier to transfer between the hydrothermal coating and Hank's solution, and an electrochemical reaction occurs. The polarization resistance (R_p) is the sum of R_f and R_{ct} . The diameter of the capacitive loop is directly proportional to the R_p . Thus, the EIS plots clearly reveal a larger R_p for the coated AZ31 than the uncoated one and the pH=10-treated AZ31 has the largest R_p of 78 677 Ω .

The Bode plots of Fig.4b shows that the impedance modulus and the phase angle of the hydrothermally treated specimens are higher than those of the untreated AZ31. The phase angle of the pH=6-treated specimen is close to 40°, lower than that of the other specimens, which may also be

caused by the micro-pores of the coating. Other hydrothermally treated specimens have a wider range of frequencies than the untreated AZ31. Moreover, the pH=10-treated AZ31 specimen has the highest impedance modulus. It reveals that the coating on pH=10-treated AZ31 is an effective physical barrier to corrosion in Hank's solution.

2.2.2 Immersion test

Fig.6 is the volume of hydrogen gas in Hank's solutions for the AZ31 substrate and the coated specimens. For the uncoated AZ31, the volume of hydrogen is about 2.6 mL after 15 d immersion. The hydrogen volume of the hydrothermally treated AZ31 at pH=6, 8 and 10 after 15 d immersion are only 0.3, 0.4 and 0.2 mL, respectively, much lower than that of the untreated substrate.

Fig.7 displays the surface macrographs of untreated and hydrothermally treated AZ31 specimens after 15 d immersion in Hank's solution. The untreated AZ31 exhibits obvious corrosion pits on the edge and large areas of filiform corrosion (Fig.7a). The pH=8-treated specimen shows obvious corrosion spots which also distributes on the edge (Fig.7c). The corrosion may be caused by the defects of coating, which often appears at the edge of the specimen. No visible corrosion spots are observed on the pH=6 and pH=10 treated AZ31.

Fig.8 shows the SEM micrographs of the specimens. The chemical components of the corresponding areas in Fig.8 obtained by EDS are listed in Table 4. Fig.8a shows that the naked AZ31 is covered by a reaction layer and lots of cracks are found on the surface. Table 4 shows that besides Mg and O, significantly high contents of P (7.18 at%) and Ca (6.11 at%)

Table 3 Parameters of equivalent circuit

Sample	$R_s/\Omega\cdot\text{cm}^2$	$Q_1/\times 10^{-6}\text{F}\cdot\text{cm}^{-2}$	n_1	$R_f/\Omega\cdot\text{cm}^2$	$Q_2/\times 10^{-6}\text{F}\cdot\text{cm}^{-2}$	n_2	$R_{ct}/\Omega\cdot\text{cm}^2$	$R_p (R_p=R_f+R_{ct})/\Omega\cdot\text{cm}^2$
AZ31	151.7	7.96	0.95	4343	611	0.40	2252	6595
pH=6-treated	139.2	6.28	0.61	7078	8.94	0.66	148	7226
pH=8-treated	138.5	9.10	0.65	45210	1.77	0.82	247	45457
pH=10-treated	131.8	8.63	0.62	77950	7.15	0.72	727	78677

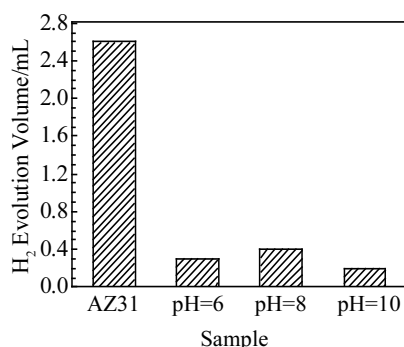


Fig.6 Hydrogen evolution volume of the AZ31 and hydrothermally treated AZ31 at various pH values in Hank's solution for 15 d

on area 1 are detected, which means that calcium phosphate is formed while the Mg substrate is corroded. Specimens treated at pH=6 and pH=10 show that most of the coating are intact except a very small part of the coating damaged (marked in area 2 and area 6). EDS results on these damaged areas show a significantly high contents of P and Ca compare with the substrate (area 1). The reason may be that there is an ionic bond of Mg^{2+} and PO_4^{3-} at the interface between the initial sediments and the AZ31 substrate, which will cause a strong combination of the inner calcium phosphate layer. Fig.8c shows the corrosion spots of the pH=8-treated specimen (marked in Fig.7c), suggesting that part of the HA layer has fallen off and a large amount of Mg (21.26 at%) and 1.76 at% Al are detected (marked in area 4).

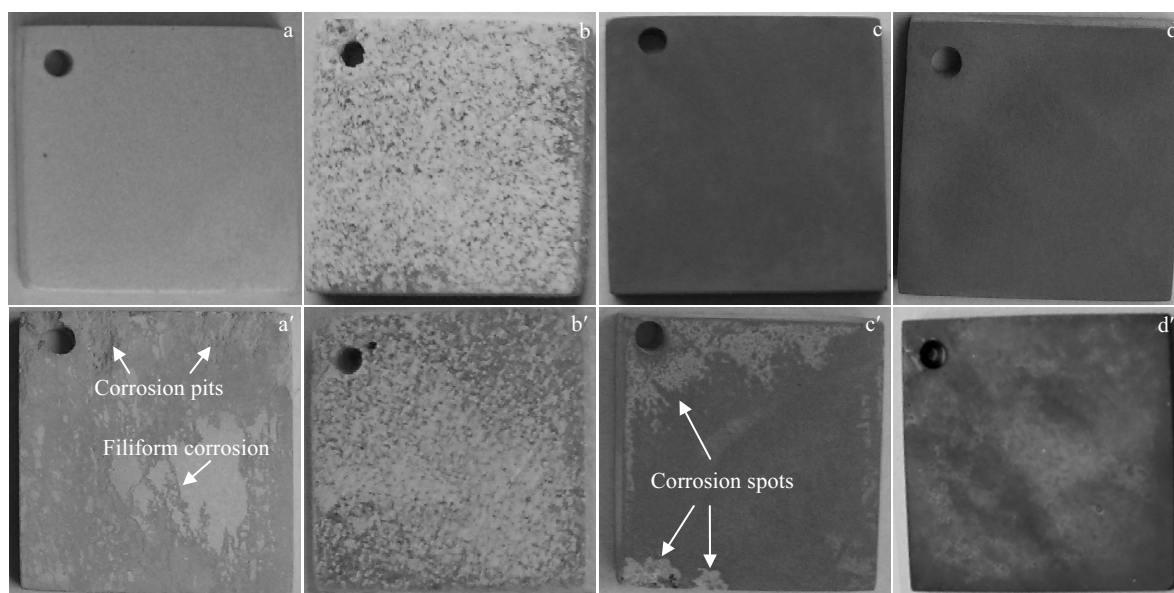


Fig.7 Macrographs of the AZ31 alloy and hydrothermally treated samples before (a~d) and after (a'~d') hydrogen evolution test in Hank's solution: (a, a') AZ31, (b, b') pH=6, (c, c') pH=8, and (d, d') pH=10

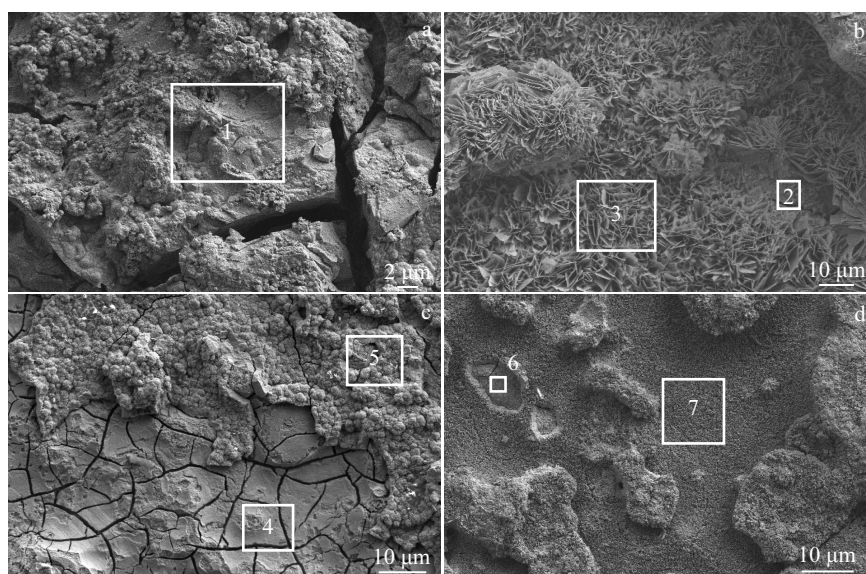


Fig.8 SEM images of AZ31 alloy (a) and hydrothermally treated samples (b~d) after hydrogen evolution test in Hank's solution: treated at pH=6 (b), pH=8 (c), and pH=10 (d)

Table 4 EDS results of the areas marked in Fig.8 (at%)

Marked area	O	Na	Mg	Al	P	Ca
1	55.53		30.03	1.14	7.18	6.11
2	58.90	1.03	3.83		17.59	16.94
3	55.32	1.98	0.38		17.10	25.21
4	57.69	2.09	21.26	1.76	10.90	6.31
5	63.93	1.88	3.82		13.65	16.72
6	58.02	1.69	5.96		13.29	20.02
7	58.20	2.67	1.13		15.89	22.11

3 Conclusions

1) Calcium phosphate coatings can be formed on AZ31 alloys by hydrothermal deposition in the 0.25 mol/L Ca-EDTA/0.25 mol/L KH_2PO_4 solution with a pH value of 6, 8 and 10. The pH values of the solution influences the phase composition and microstructure of the coatings. The deposited Ca-P coating treated at pH=6 consists of OCP. When the pH values increase to 8 and 10, only the HA forms on the AZ31 alloy.

2) The calcium phosphate coatings improve the corrosion resistance property of AZ31 alloys. The degree of protection provided by the Ca-P coating varies with its microstructure. The pH=10-treated AZ31 with nano-scale and dense rod-like HA crystals has the largest R_p and the lowest i_{corr} . After immersion in Hank's solution for 15 d, most of the coating formed on pH=10-treated AZ31 is intact. The HA coating with rod-like crystals can prevent the penetration of solution more effectively than the micrometer scale lamellar-like OCP (pH=6) and honeycomb-like HA coating (pH=8).

References

- Witte F, Hort N, Vogt C et al. *Current Opinion in Solid State and Materials Science*[J], 2008, 12(5-6): 63
- Xin Y, Hu T, Chu P K. *Acta Biomaterialia*[J], 2011, 7(4): 1452
- Waizy H, Seitz J M, Reifemath J et al. *J Mater Sci*[J], 2013, 8(1): 39
- Zeng R C, Dietzel W, Witte F et al. *Adv Eng Mater*[J], 2008, 10(8): 3
- Wan P, Tan L L, Yang K. *Journal of Material Science & Technology*[J], 2016, 32(9): 827
- Renato A A, Marac C L. *Acta Biomaterialia*[J], 2012, 8(3): 937
- Agarwal S, Curtin J, Duffy B et al. *Materials Science and Engineering C*[J], 2016, 68 (11): 948
- Li X, Liu X M, Wu S L et al. *Acta Biomaterialia*[J], 2016, 12(11): 2
- Dorozhkin V S. *Acta Biomaterialia*[J], 2014, 10(7): 2919
- Hiromoto S, Tomozawa M. *Surface & Coatings Technology*[J], 2011, 205(17): 4711
- Chen Z T, Mao X L, Tan L L. *Biomaterials*[J], 2014, 35(30): 8553
- Tomozawa M, Hiromoto T S. *Acta Materialia*[J], 2011, 59(1): 355
- Cheng Z J, Lian J S, Hui Y X et al. *Journal of Bionic Engineering*[J], 2014, 11(4): 610
- Wang H, Zhu S, Wang L et al. *Applied Surface Science*[J], 2014, 307(6): 92
- Yang J X, Jiao Y P, Cui F Z et al. *Surface & Coatings Technology*[J], 2008, 202(22): 5733
- Tang H, Gao Y. *Journal of Alloys & Compounds*[J], 2016, 688(12): 699
- Kannan M B. *Surface & Coatings Technology*[J], 2016, 301(9): 36
- Zhang C Y, Zeng R C, Liu C L et al. *Surface & Coatings Technology*[J], 2010, 204(21-22): 3636
- Waterman J, Pietak A, Birbilis N et al. *Materials Science and Engineering B*[J], 2011, 176(20): 1756
- Falahieh S K, Nemeth S, Tan M J. *Surface & Coatings Technology*[J], 2014, 258 (11): 931
- Tomozawa M, Hiromoto S, Harad Y. *Surface & Coatings Technology*[J], 2010, 204 (20): 3243
- Hiromoto S, Tomozawa M. *Surface & Coatings Technology*[J], 2011, 205(19): 4711
- Laquerriere P, Laquerriere A G, Jallot E et al. *Biomaterials*[J], 2003, 24(16): 2739
- Li B, Guo B, Fan H et al. *Applied Surface Science*[J], 2008, 255(2): 357
- Han Y, Xu K W. *Mater Sci Mater Med*[J], 1999, 10(4): 243
- Johnsson M S, Nancollas G H. *Critical Reviews in Oral Biology and Medicine*[J], 1992, 3(1): 361
- Tomozawa M, Hiromoto S. *Acta Materialia*[J], 2011, 59(1): 355
- Venugopal A, Raja V S. *Corros Sci*[J], 1997, 39(12): 2053

pH 值对镁合金表面水热沉积磷酸钙涂层微观形貌和腐蚀性能的影响

张春艳^{1,2}, 张世雨¹, 柳歆鹏¹, 何洪川¹

(1. 重庆理工大学, 重庆 400054)

(2. 重庆市特种焊接材料与技术高校工程研究中心, 重庆 400054)

摘要: 为改善镁合金的耐蚀性和生物相容性, 采用水热法在不同 pH 值条件下于 AZ31 镁合金表面制备了磷酸钙 (Ca-P) 涂层。利用 XRD、SEM 和 EDS 分析了不同 pH 值下涂层的物相组成、微观形貌和化学成分; 在 Hank's 仿生溶液中采用电化学测试和浸泡的方法研究了涂层的生物腐蚀行为。结果表明: 水热处理的 pH 值影响涂层的相组成和微观形貌, 涂层的微观形貌影响涂层的防护性能。当 pH 值为 6 时, Ca-P 涂层由 OCP ($\text{Ca}_8\text{H}_2(\text{PO}_4)_6 \cdot 5\text{H}_2\text{O}$) 组成, 当 pH 值增加到 8 和 10 时, Ca-P 涂层为羟基磷灰石 (HA)。pH 值为 8 时, HA 涂层呈蜂窝状; pH 值为 10 时, HA 涂层由纳米尺度的棒状晶体构成, 该涂层在 Hank's 溶液中能有效阻止溶液的渗透而保护基体。
关键词: Ca-P 涂层; 镁合金; 水热沉积; 腐蚀性能; 生物材料

作者简介: 张春艳, 女, 1974 年生, 博士, 副教授, 重庆理工大学材料科学与工程学院, 重庆 400054, 电话: 023-62563178, E-mail: zhangchunyan@cqut.edu.cn